Supporting Information

Lamellar Porous Vermiculite Membranes for Boosting Nanofluidic Osmotic Energy Conversion

Li Cao[a,b], Hong Wu[a,b,c*], Chunyang Fan[a,b], Zhiming Zhang[a,b], Benbin Shi[a,b], Pengfei Yang[a,b], Ming Qiu[a,b], Niaz Ali Khan[a,b] and Zhongyi Jiang[a,b,d*]

a Key Laboratory for Green Chemical Technology of Ministry of Education, School of Chemical Engineering and Technology, Tianjin University, Tianjin 300072, China

b Collaborative Innovation Center of Chemical Science and Engineering (Tianjin), Tianjin 300072, China

c Tianjin Key Laboratory of Membrane Science and Desalination Technology, Tianjin University, Tianjin 300072, China

d Joint School of National University of Singapore and Tianjin University, International Campus of Tianjin University, Binhai New City, Fuzhou, 350207, China

Experimental

Preparation of porous vermiculite nanosheets and lamellar membranes.

Vermiculite nanosheets were synthesized by an ion-exchange method from thermally expanded vermiculite powders as reported previously[1,2]. Porous vermiculite nanosheets were then synthesized by chemical etching the exfoliated vermiculite nanosheets using hydrochloride acid. Typically, 0.5 g of vermiculite nanosheets colloids were added in 100 mL hydrochloride acid solution with a specific concentration at 60 ^{o}C and stirred for 6 h, followed by centrifugation at 12000 rpm for 30 min and repeated washing using deionized water until pH around 7. A porous vermiculite nanosheets suspension of 0.5 mg mL^{-1} were obtained after re-dispersing the precipitated colloids in deionized water. The pore size in the vermiculite nanosheets was tuned by altering the concentration of hydrochloride acid from 0.2 to 0.8 M, and the corresponding porous vermiculite nanosheets are denoted as PV-x nanosheets, where x represents the concentration of hydrochloride acid. The lamellar porous vermiculite membranes (PVM-x) were fabricated by filtering PV-x nanosheets dispersion on a polyethersulfone microporous membrane (pore size: 0.22 μm, diameter: 47 mm). Finally, the PVM-x were further cross-linked in a glutaraldehyde vapor at 80 ^{o}C for 24 h and were dried at 60 ^{o}C for 12h. A free-standing PVM can be obtained by dissolving the polyethersulfone support in N, N-dimethylformamide and then dried at 60 ^{o}C for 12 h.

Characterization of porous vermiculite nanosheets and membranes

The microstructures of porous vermiculite nanosheets and membranes were characterized by a field emission scanning electron microscope (FESEM, Nanosem 430) and transmission electron microscope (TEM, Tecnai G2 F20) with an acceleration voltage of 200 kV. The surface morphology and nanosheets thickness were determined using an atomic force microscopy (AFM, BRUKER Dimension Icon). The Zeta potential of porous vermiculite nanosheets was performed using a Malvern Zetasizer Nano ZS90 at various pH values. X-ray diffraction (XRD) patterns of wet membranes were recorded on a D/MAX-2500 X-ray diffractometer (Cu Kα radiation). All membranes were soaked in deionized water for 12 h before XRD test.

Electrical measurements

The PVMs were mounted in a custom-made electrochemical cell. The transmembrane ion transport of the PVMs were performed by taking the I-V characteristics in various concentration KCl solutions, using an impedance/gain-phase analyzer (PARSTAT4000) at room temperature (25±2 °C). A pair of Ag/AgCl electrodes was used to apply bias voltage and collect current signals. To measure osmotic energy conversion, one chamber was filled with 1 mM KCl solution (C_{low}), the concentration of KCl (C_{high}) in the other chamber varied from 10 mM to 1 M. Then the I-V characteristics were recorded, from which the open-circuit voltage (interception at zero current) and short-circuit current (interception at zero voltage) could be obtained. The generated osmotic voltage and osmotic current were obtained by subtracting the contribution from the redox potential on Ag/AgCl electrodes in different concentrations. For all electrical measurements, the effective testing area of PVMs are about 0.01 and 0.03 mm^2, which is similar to that reported in other previous works[3,4].

Ion selectivity and energy conversion efficiency calculation

The ion selectivity of ions can be quantitively described by the transference number t, which is calculated by the following equation[3],

$$t = \frac{1}{2}\left[\frac{V_{OS}}{\frac{RT}{zF} ln \frac{\lambda_{C_H} C_H}{\lambda_{C_L} C_L}} + 1\right]$$

where V_{OS} is the generated osmotic potential; R, T, z, F are the gas constant, temperature, valence charge and Faraday constant, respectively; λ and C represent the ion activity coefficient and ion concentration, respectively.

The energy conversion efficiency can be calculated as,

$$\eta = \frac{(2t - 1)^2}{2}$$

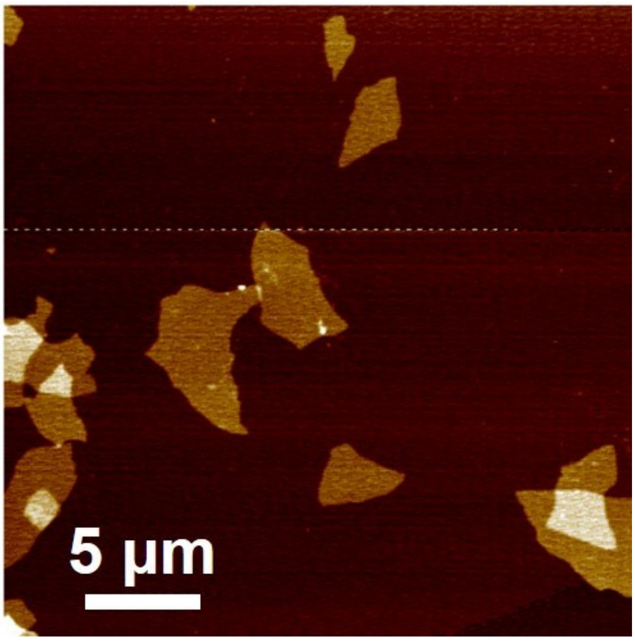

Fig. S1 AFM image of vermiculite nanosheets

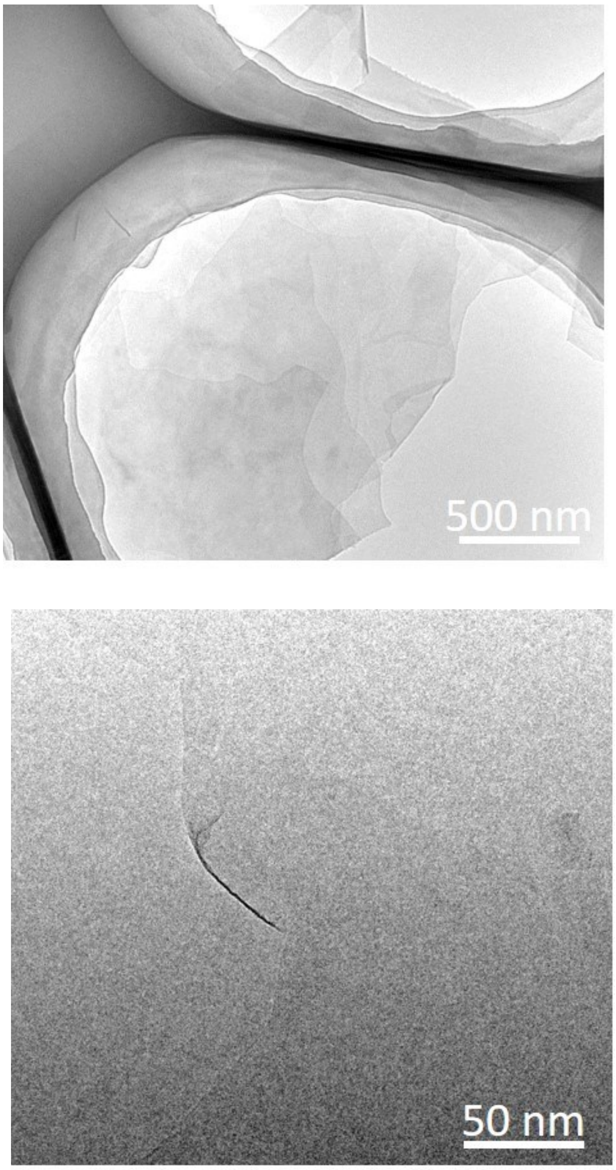

Fig. S2 TEM images of vermiculite nanosheets.

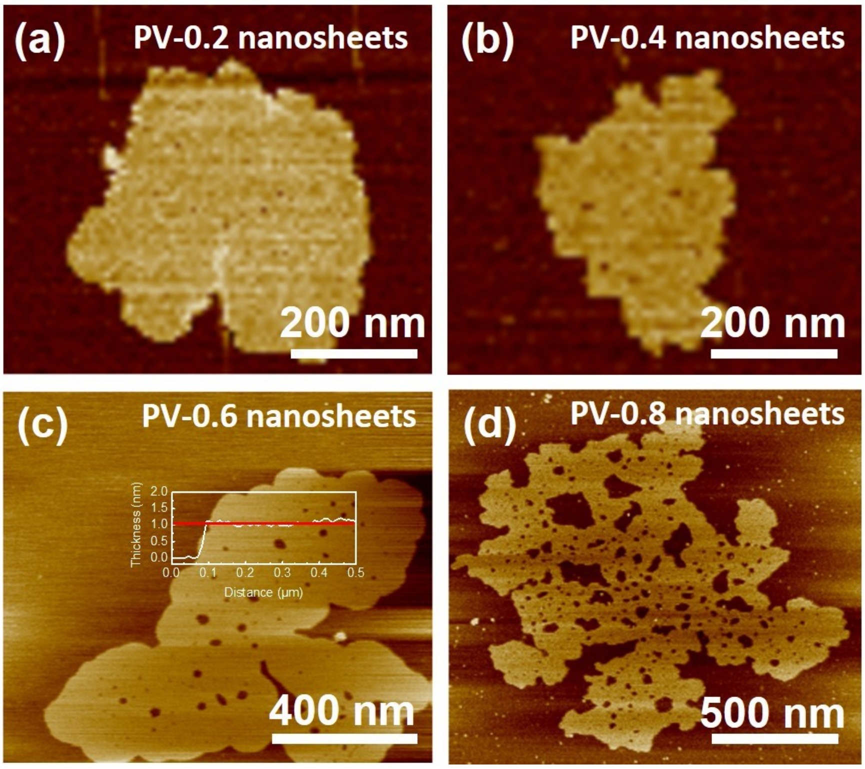

Fig. S3 AFM images of porous vermiculite nanosheets. The PV nanosheets have a thickness of ~1 nm, indicating a monolayer.

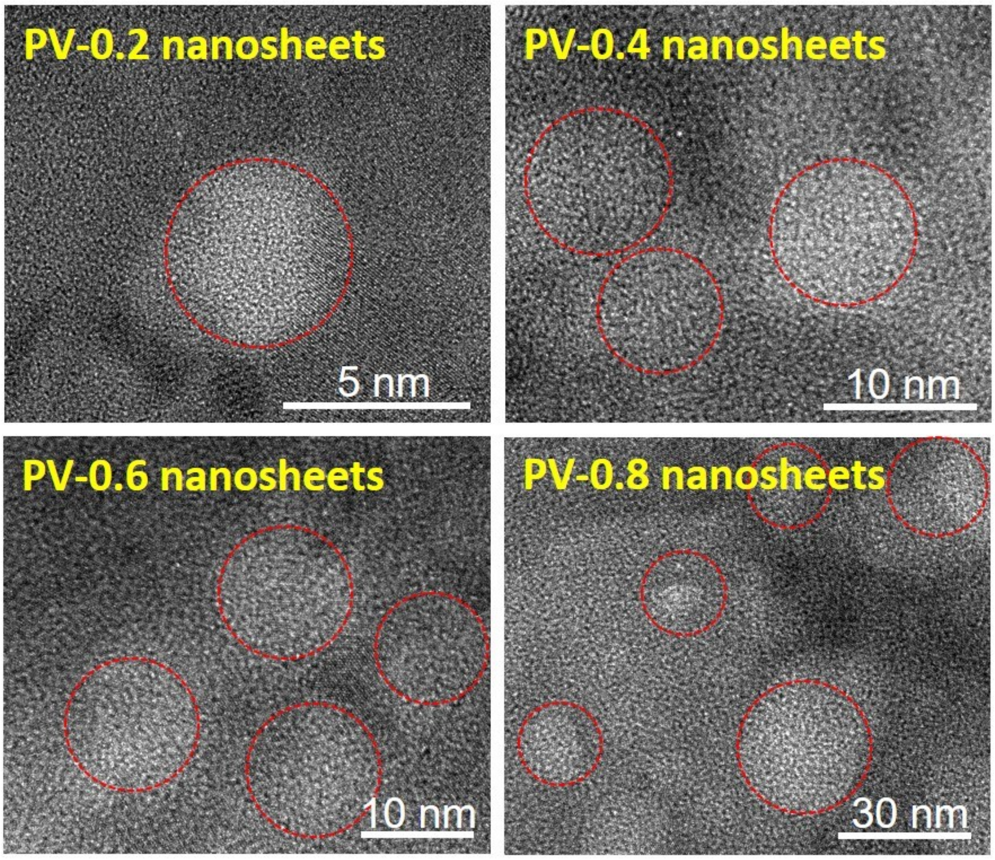

Fig. S4 TEM images of porous vermiculite nanosheets. The red dash circles highlight the nanopores in basal plane of vermiculite nanosheets.

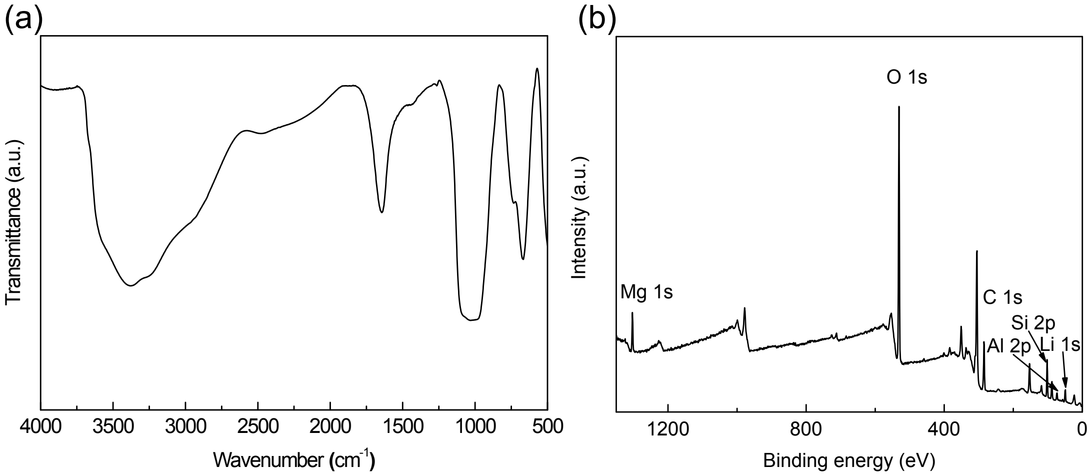

Fig. S5 FTIR and XPS spectra of porous vermiculite membranes. Fig. S5a shows FTIR spectrum of porous vermiculite membranes. The strong bands at around 3400-3450 and 1643 cm^{-1} attributed to the O-H stretching vibration of water. The characteristic band at 995-1100 cm-1 is attributed to the Si-O-Si and Si-O-Al stretching vibrations. The chemical composition of vermiculite was further characterized using XPS, as shown in Fig. S5b. The XPS spectrum shows the presence of Mg, O, Al, Si, which are the constitutive elements of vermiculite materials. The presence of C and Li elements can be ascribed to the cross-linker and intercalated lithium ions, respectively.

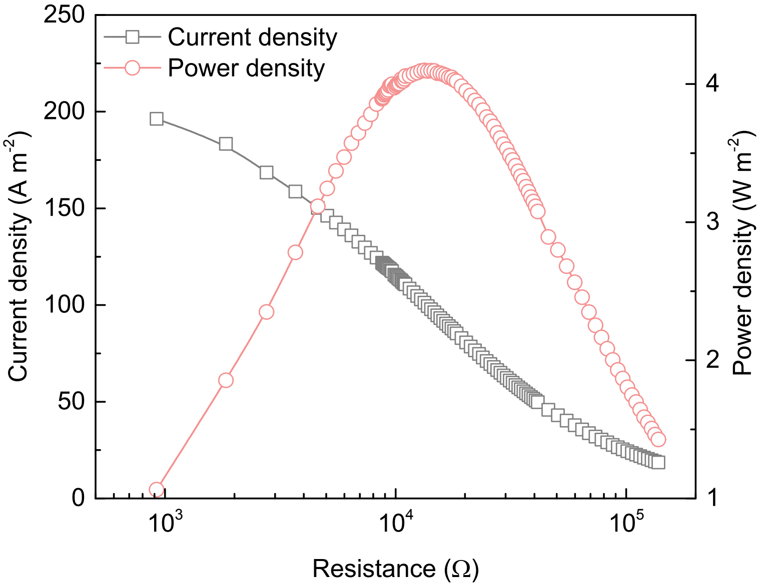

Fig. S6 Power generation of a PVM-0.6 membrane (the effective testing membrane area is 0.03 mm^2) by mixing artificial sea water (0.5M NaCl) and river water (0.01M NaCl).

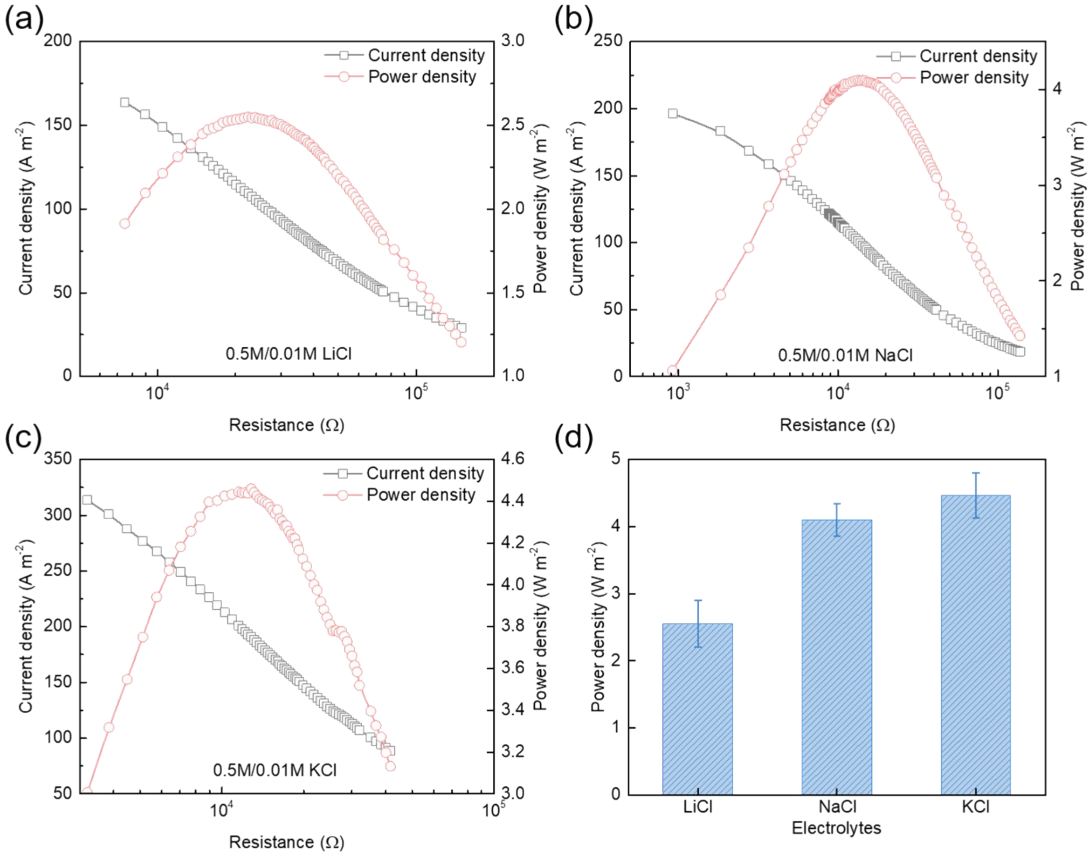

Fig. S7 Power density of PVM-0.6 under various salt electrolytes (The effective testing membrane area was 0.03 mm^2).

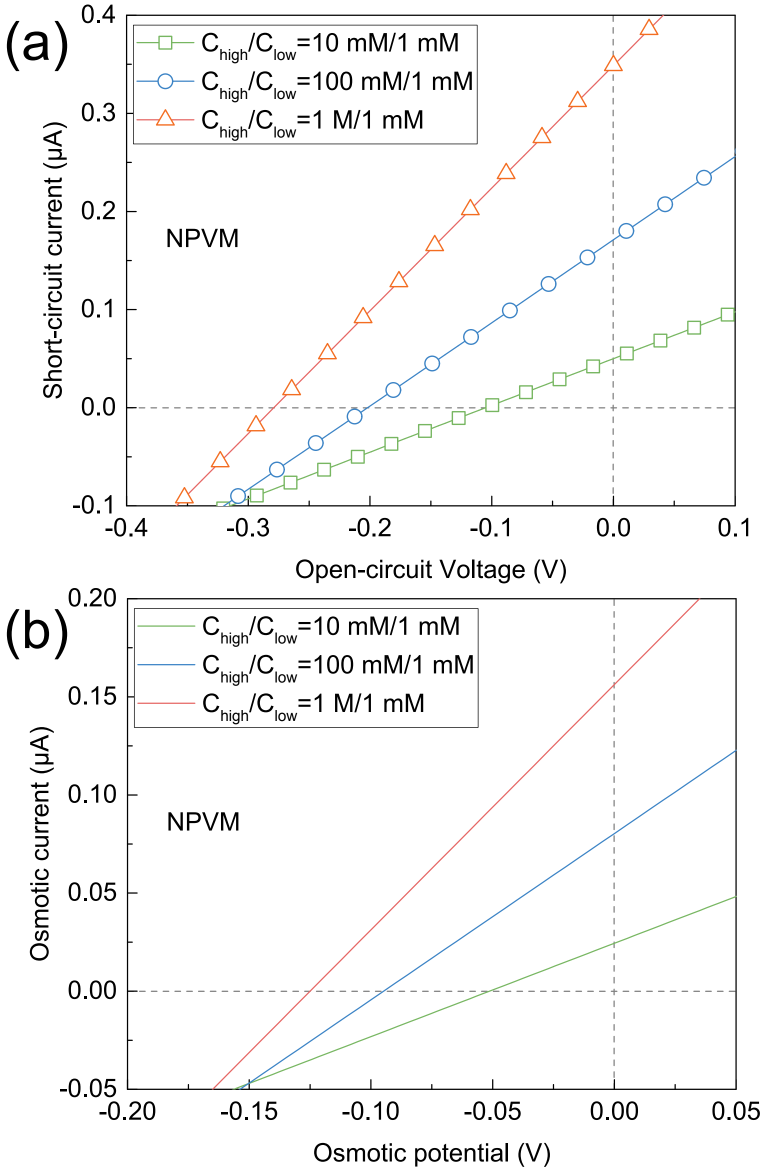

Fig. S8 I-V curves of NPVM under various concentration gradients. a) short-circuit current vs open-circuit voltage, b) osmotic current vs osmotic potential.

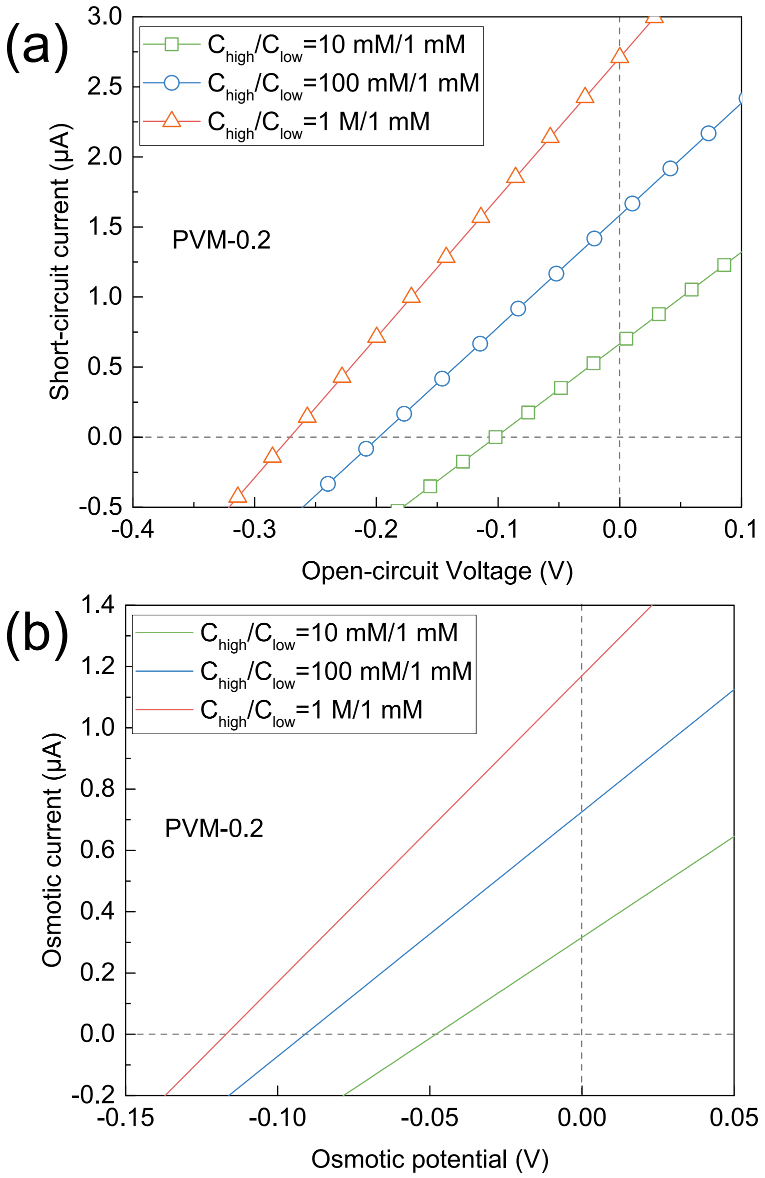

Fig. S9 I-V curves of PVM-0.2 under various concentration gradients. a) short-circuit current vs Open-circuit voltage, b) osmotic current vs osmotic potential.

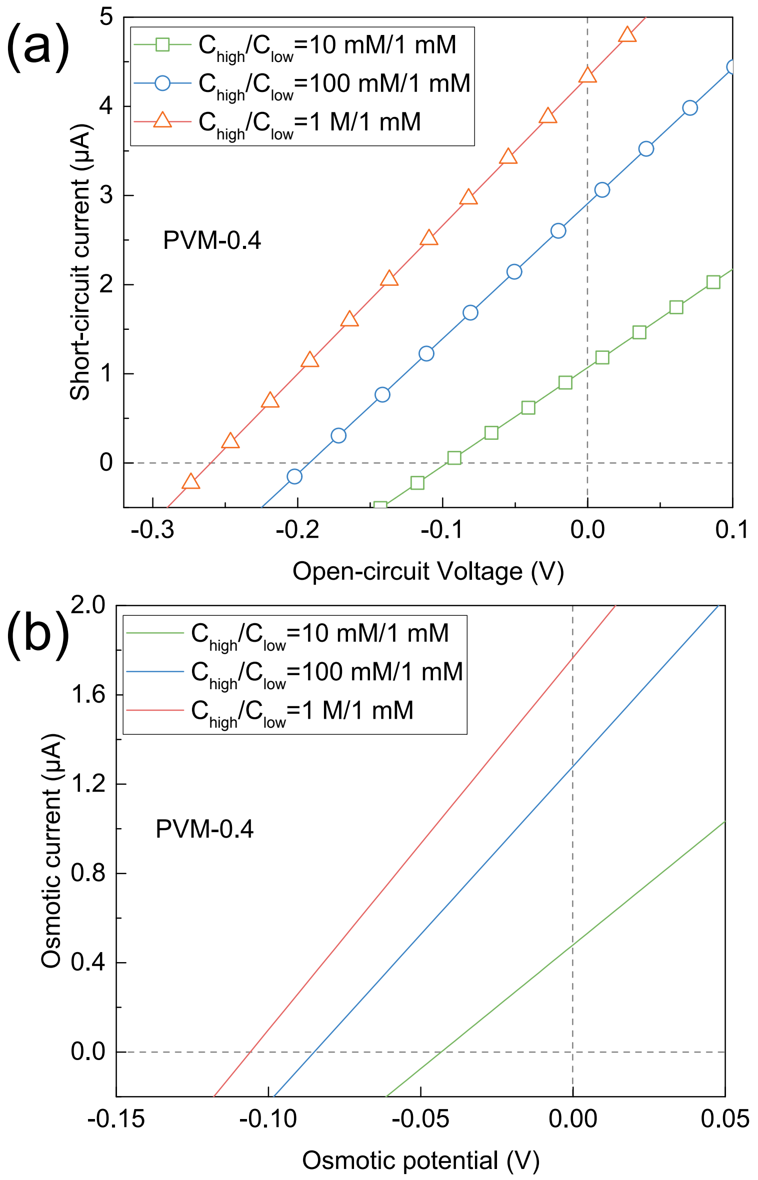

Fig. S10 I-V curves of PVM-0.4 under various concentration gradients. a) short-circuit current vs Open-circuit voltage, b) osmotic current vs osmotic potential.

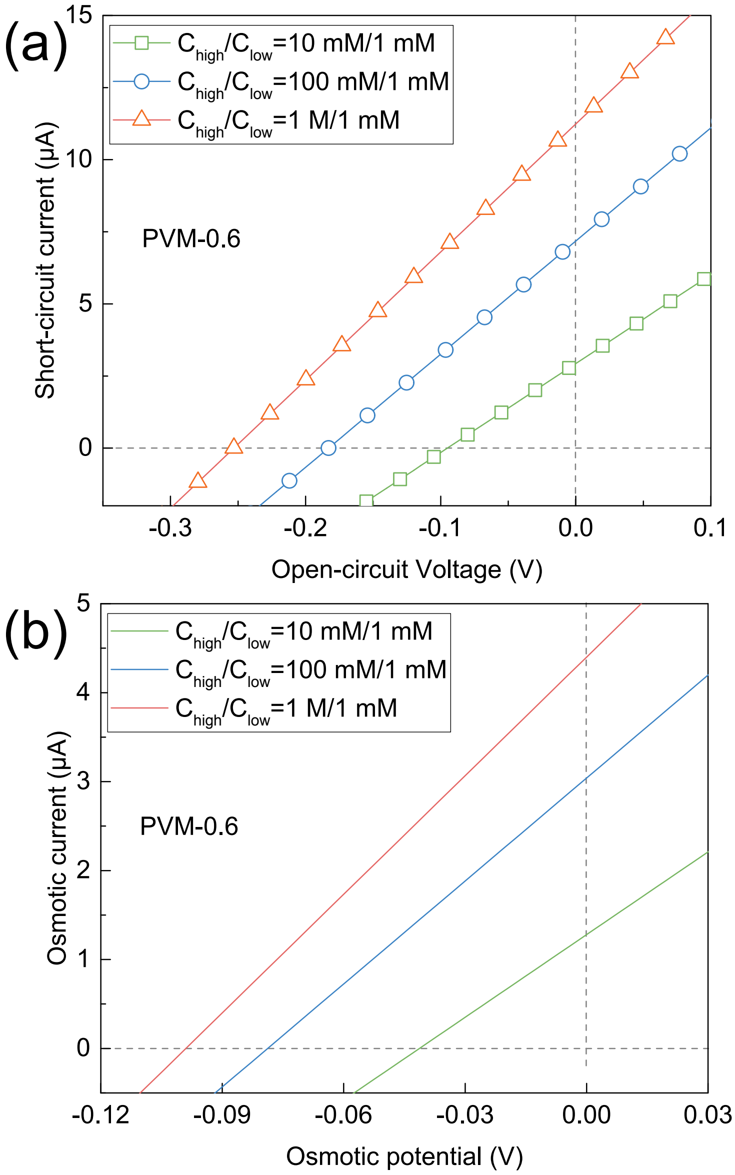

Fig. S11 I-V curves of PVM-0.6 under various concentration gradients. a) short-circuit current vs Open-circuit voltage, b) osmotic current vs osmotic potential.

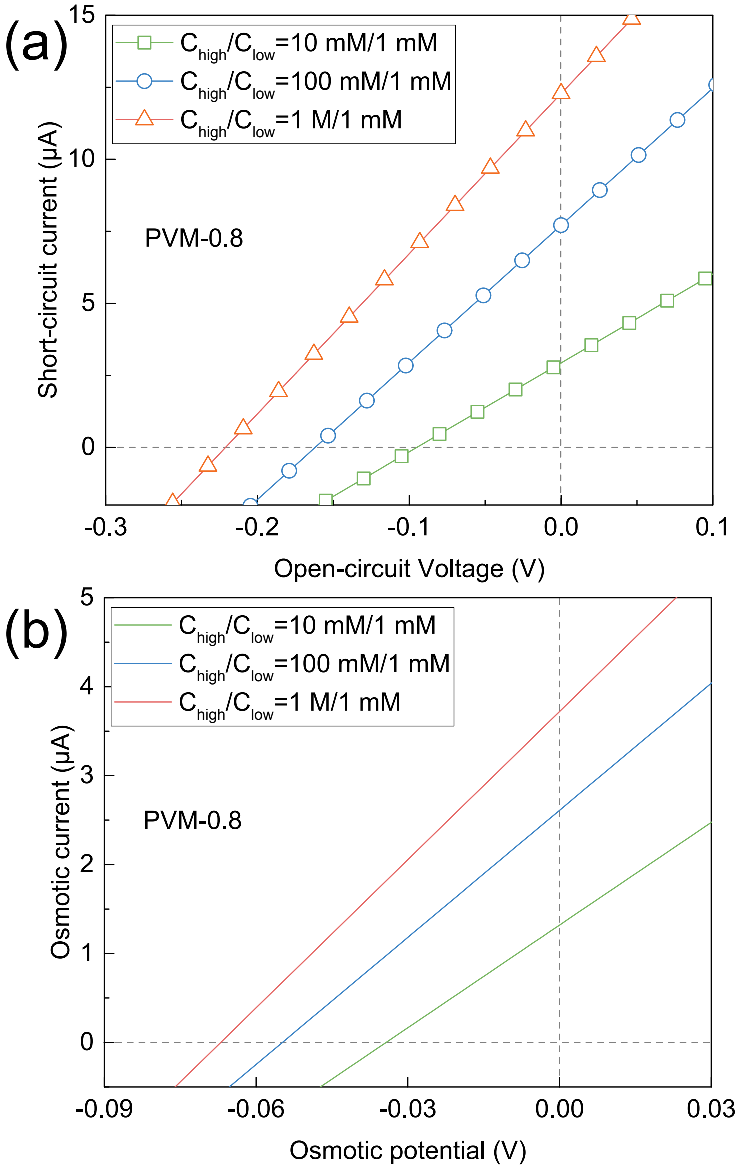

Fig. S12 I-V curves of PVM-0.8 under various concentration gradients. a) short-circuit current vs Open-circuit voltage, b) osmotic current vs osmotic potential.

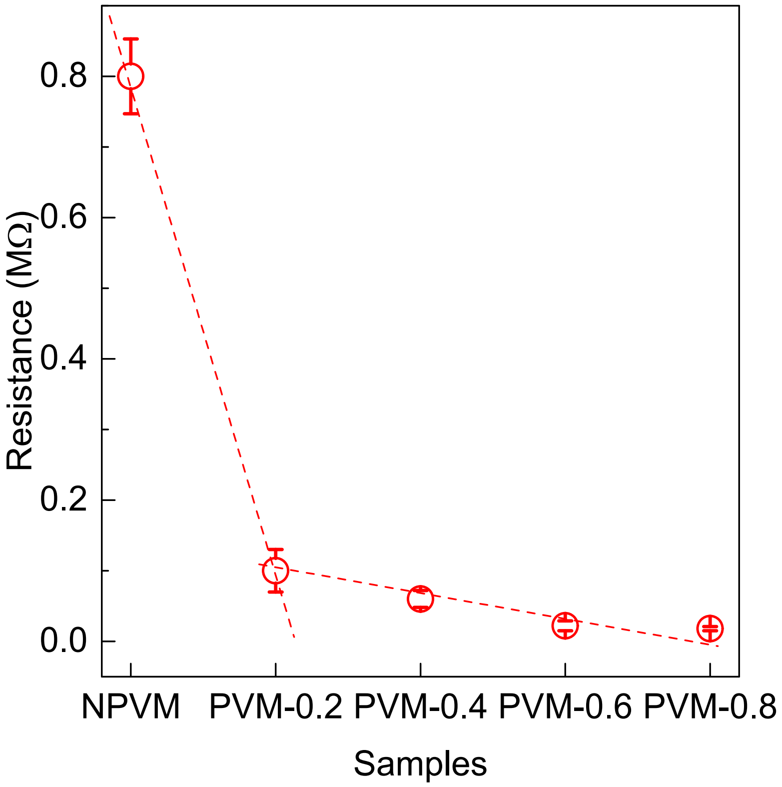

Fig. S13 Internal resistance of NPVM and PVMs under 1M/1mM KCl solution.

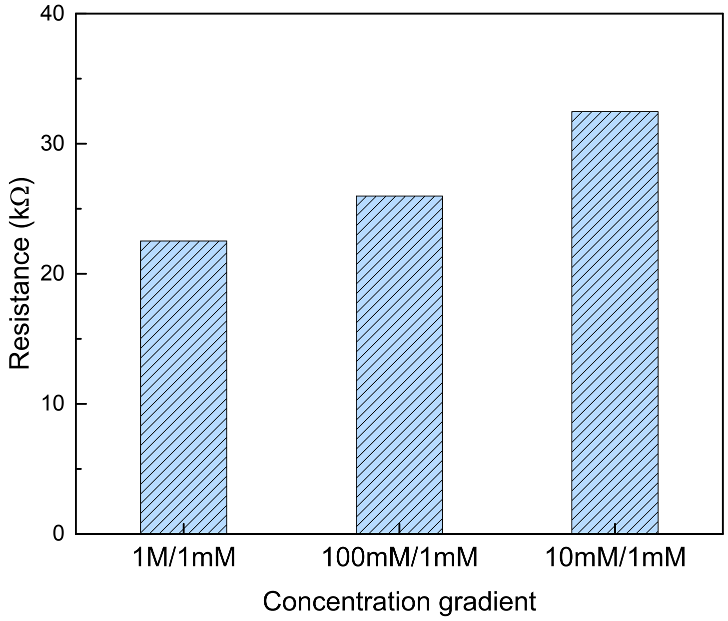

Fig. S14 Internal resistance of PVM-0.6 membrane at various concentration gradient.

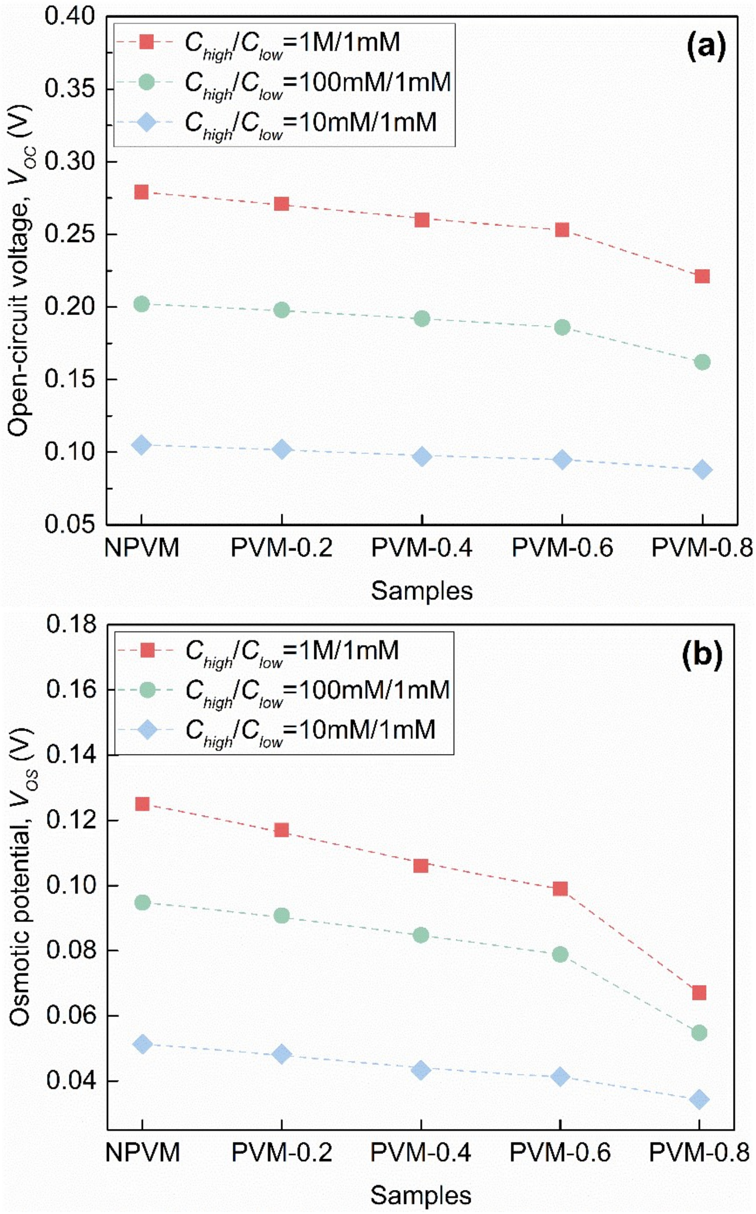

Fig. S15 Open-circuit voltage (a) and the generated osmotic potential (b) for PVMs with various pore size.

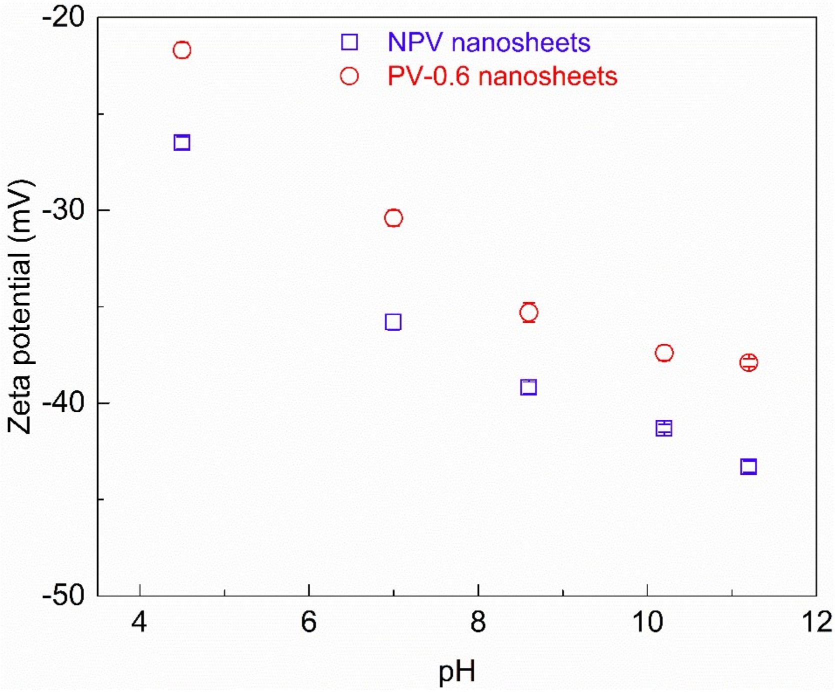

Fig. S16 Zeta potential of nonporous vermiculite nanosheets and porous vermiculite nanosheets under varied pH values.

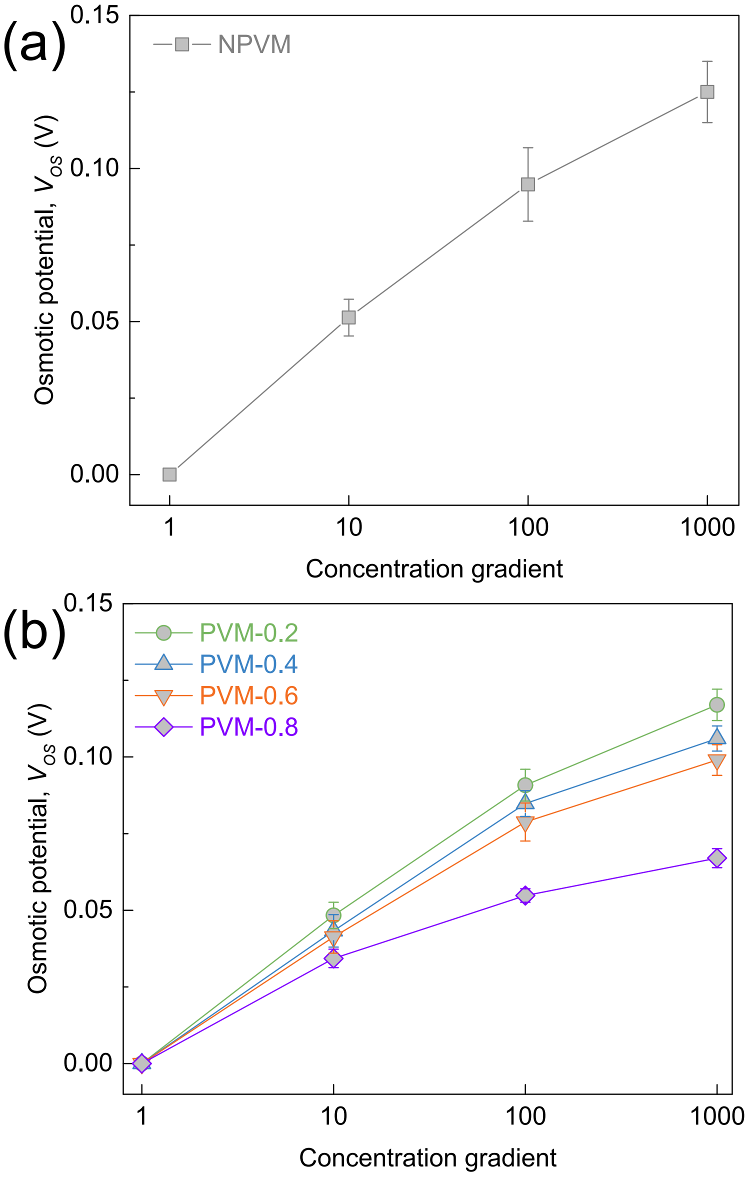

Fig. S17 The generated osmotic potential for NPVM (a) and PVMs (b) under different concentration gradients.

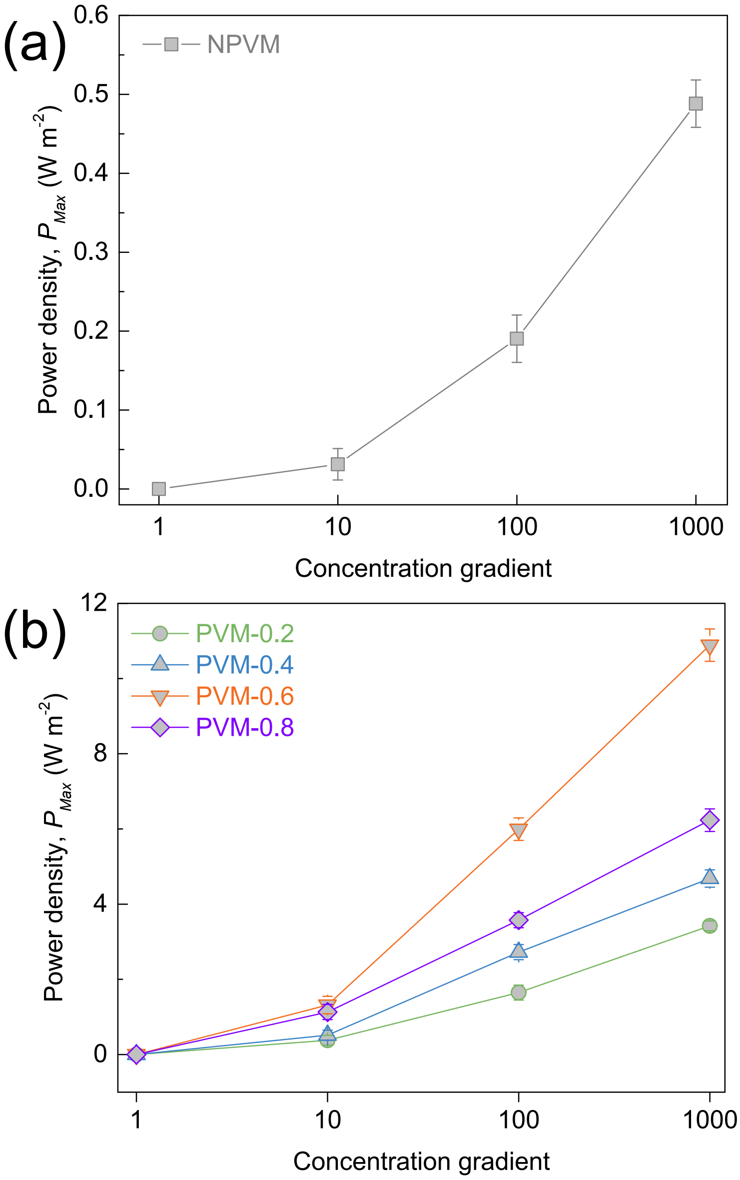

Fig. S18 Output power density for NPVM (a) and PVMs (b) under different concentration gradients.

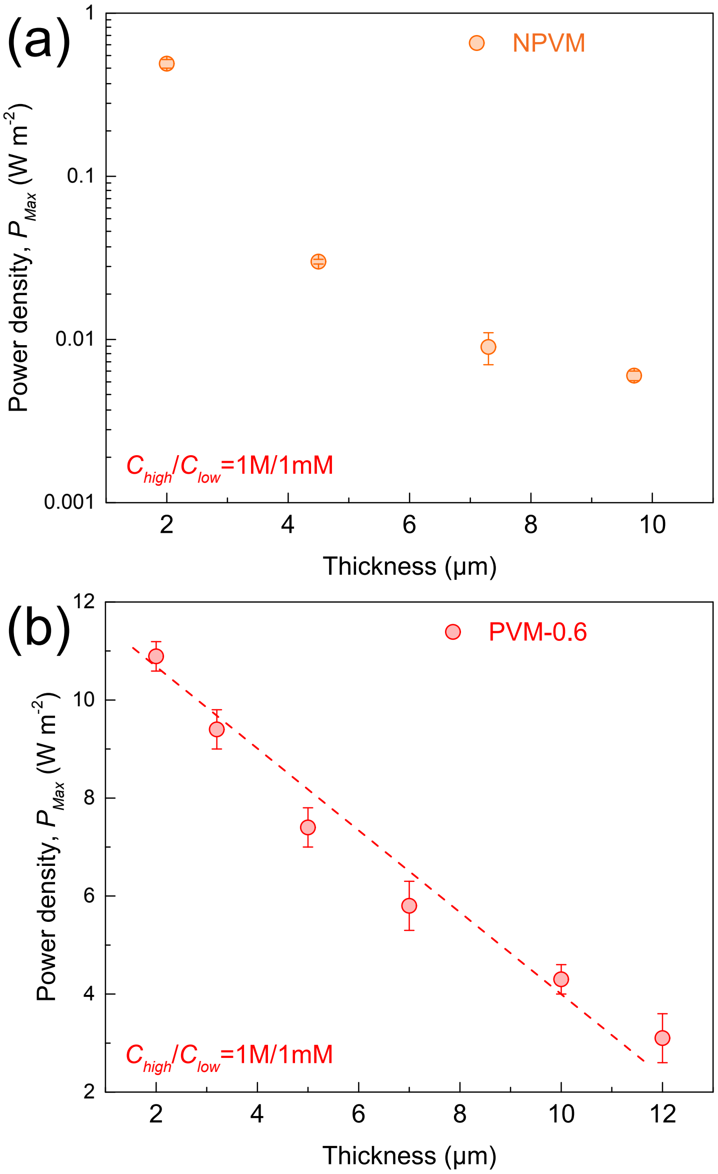

Fig. S19 Out power density versus thickness of NPVM (a) and PVMs (b) under a KCl concentration gradient of 1000.

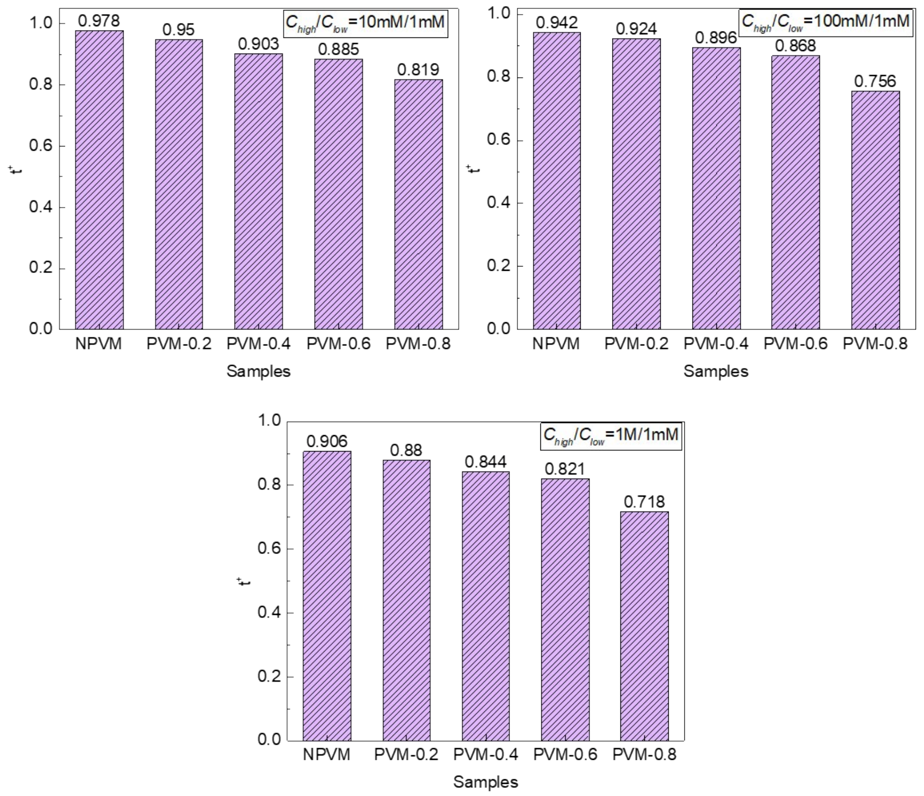

Fig. S20 Ion transference numbers of PVMs under various concentration gradients.

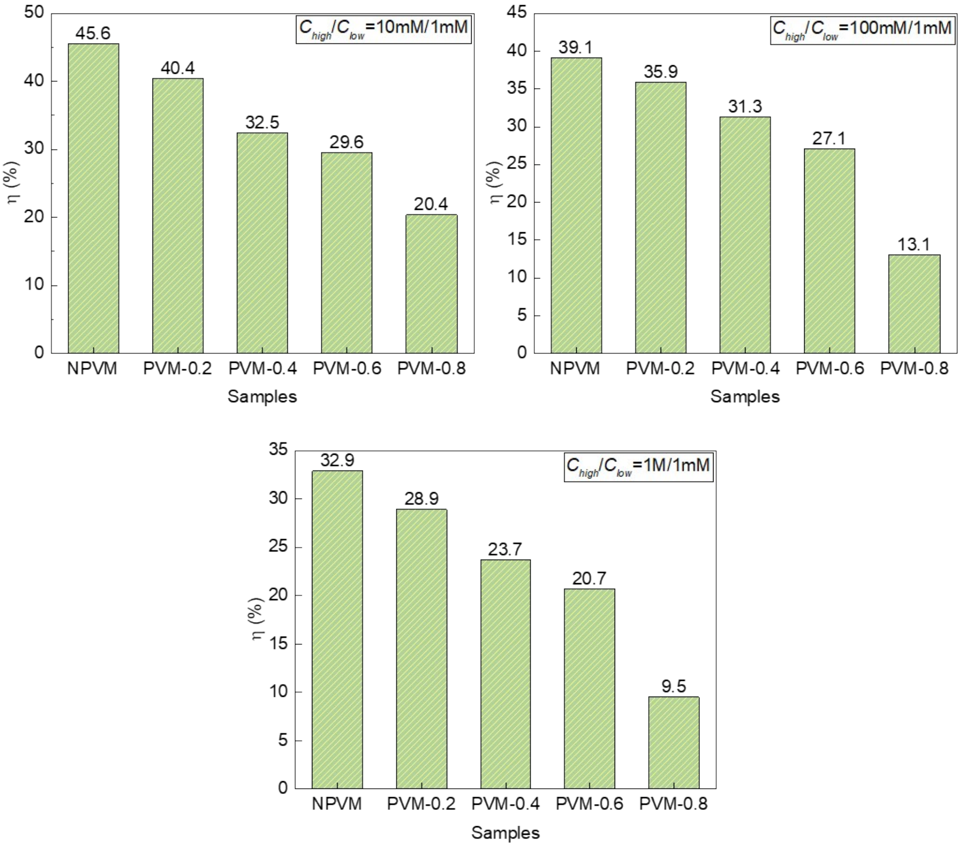

Fig. S21 Energy conversion efficiency of PVMs under various concentration gradients.

Supplementary Tables

Table S1. Comparison of the output power density of representative membranes reported in the literatures and in this study.

Membrane types	Concentration gradient	P_{Max} (W m^{-2})	References
Polycarbonate track-etch membranes	1 M/1mM	0.058	[5]
2D kaolinite	0.1 M/1mM	0.18	[6]
Polymeric-C3N4	0.1 M/0.1mM	0.21	[7]
Graphene oxide membrane	0.5 M/10mM	0.77	[8]
Janus three-dimensional (3D) porous membrane	0.5 M/10mM	2.66	[9]
Silk-based hybrid membranes	0.5 M/10mM	2.86	[10]
PSS/MOF	0.5 M/10mM	2.87	[11]
ionic diode membrane	0.5 M/10mM	3.46	[12]
MXene/Kevlar membranes	0.5 M/10mM	3.7	[3]
Vertically transported MXene membranes	0.5 M/10mM	4.6	[13]
Vertically transported graphene oxide membranes	0.5 M/10mM	10.6	[14]
Lamellar porous vermiculite membranes	0.5 M/10mM	4.5[a]	This work
	1 M/1mM	10.9[a]	
	0.5 M/10mM	4.1[b]	
	1 M/1mM	9.7[b]	

[a] The effective testing membrane area is 0.01 mm^2.

[b] The effective testing membrane area is 0.03 mm^2.

Table S2. Redox potential values for various C_{high}/C_{low}

C_{high}/C_{low}	10mM/1mM	100mM/1mM	1M/1mM
Eredox (mV)	53.7	107.2	154.1

Supplementary references

1 L. Cao; H. Wu; X. He; H. Geng; R. Zhang; M. Qiu; P. Yang; B. Shi; N. A. Khan and Z. Jiang, *J. Mater. Chem. A,* 2019, **7**, 25657-25664.

2 J.-J. Shao; K. Raidongia; A. R. Koltonow and J. Huang, *Nat. Commun.,* 2015, **6**, 7602.

3 Z. Zhang; S. Yang; P. Zhang; J. Zhang; G. Chen and X. Feng, *Nat. Commun.,* 2019, **10**, 2920.

4 Z. Zhang; P. Zhang; S. Yang; T. Zhang; M. Löffler; H. Shi; M. R. Lohe and X. Feng, *Proc. Natl. Acad. Sci.,* 2020, **117**, 13959-13966.

5 K. Kwon; S. J. Lee; L. Li; C. Han and D. Kim, *Int. J. Energy Res. ,* 2014, **38**, 530-537.

6 H. Cheng; Y. Zhou; Y. Feng; W. Geng; Q. Liu; W. Guo and L. Jiang, *Adv. Mater. ,* 2017, **29**, 1700177.

7 K. Xiao; P. Giusto; L. Wen; L. Jiang and M. Antonietti, *Angew. Chem. Int. Ed. ,* 2018, **57**, 10123-10126.

8 J. Ji; Q. Kang; Y. Zhou; Y. Feng; X. Chen; J. Yuan; W. Guo; Y. Wei and L. Jiang, *Adv. Funct. Mater. ,* 2017, **27**, 1603623.

9 X. Zhu; J. Hao; B. Bao; Y. Zhou; H. Zhang; J. Pang; Z. Jiang and L. Jiang, *Sci. Adv.,* 2018, **4**, eaau1665.

10 W. Xin; Z. Zhang; X. Huang; Y. Hu; T. Zhou; C. Zhu; X.-Y. Kong; L. Jiang and L. Wen, *Nat. Commun.,* 2019, **10**, 3876.

11 R. Li; J. Jiang; Q. Liu; Z. Xie and J. Zhai, *Nano Energy,* 2018, **53**, 643-649.

12 J. Gao; W. Guo; D. Feng; H. Wang; D. Zhao and L. Jiang, *J. Am. Chem. Soc. ,* 2014, **136**, 12265-12272.

13 L. Ding; D. Xiao; Z. Lu; J. Deng; Y. Wei; J. Caro and H. Wang, *Angew. Chem. Int. Ed. ,* 2020, **59**, 8720-8726.

14 Z. Zhang; W. Shen; L. Lin; M. Wang; N. Li; Z. Zheng; F. Liu and L. Cao, *Adv. Sci.,* 2020, **7**, 2000286.